

## ***Self-assembly of phenylalanine molecules under physiological conditions and its biological significance.***

Phenylalanine is known to form amyloid like higher structures which are cytotoxic. Excess accumulation of phenylalanine is known to cause Phenylketonuria (PKU), a well-known genetic abnormality, which triggers several neurological, physical and developmental severities. However, the fundamental mechanism behind the origin of such diverse health problems, particularly the issue of how they are related to the building-up of phenylalanine molecules in the body, is largely unknown.

In this work, the aggregation of phenylalanine molecules into amyloid like fibrils has been studied under physiological conditions and the effects of these phenylalanine fibrils on the aggregation propensities of selected globular proteins have also been examined. Using a combination of biophysical, molecular biology and computation tools, a systematic study on the self-assembly of phenylalanine molecules under physiological conditions and their biological significance have been investigated.

### **3.1 PHENYLALANINE FIBRIL ASSEMBLY AND ITS EFFECT ON THE AGGREGATION OF PROTEINS AND AMINOACIDS.**

The multitude of health problems associated with phenylketonuria (PKU) includes disorders such as anaemia, rickets, atopic dermatitis, coronary heart disease, diabetes mellitus and arthritis (Blau et al. 2010)(Schlegel et al. 2016)(Ruppert 1967). (Table 3.1). Though several biologically relevant inherent properties of phenylalanine have been reported including its ability to generate  $\beta$ -sheet structured higher order entities(Do et al. 2015a)(Singh et al. 2014) and cytotoxic fibrils (Adler-Abramovich et al. 2012)(Shaham-Niv et al. 2015), the question of how these diverse PKU-linked severities arise from a single defect of uncontrolled build-up of phenylalanine in the blood remains largely unanswered. This phenylalanine residue is considered as an important component of aggregation prone sequences of many amyloidogenic proteins. Table 3.2 shows the list of diseases induced by specific peptide sequences that contains aromatic residues including phenylalanine. The goal of this work was to gain insight into this fundamental question by testing whether phenylalanine fibrils would drive aggregation of globular proteins that are commonly found in the blood and by exploring what damaging effect such aggregation process would do to the RBCs whose abnormality is highly relevant to PKU.

#### **3.1.1 Self-assembly of phenylalanine molecule into amyloid like structures.**

Phenylalanine fibrils were generated by incubating  $\sim 6$  mM of phenylalanine under physiological conditions of buffer( PBS pH  $\sim 7.4$ ) and temperature( $37^\circ\text{C}$ ) (Adler-Abramovich et al. 2012). Significant rise in the fluorescence intensity of Thioflavin T, a dye that detects amyloid formation(Lee et al. 2011a), and increase in the turbidity of the sample were observed (Fig 3.1a, Fig. 3.1b), revealing the conversion of soluble phenylalanine molecules into self-assembled amyloid like higher order structures. The nature of the aggregation reaction appeared to follow a nucleation growth pathway, as no lag time was observed in a self-seeded aggregation reaction (Fig. 3.1b). SEM and AFM visualisation revealed the formation of both regular fibrils (ranging from  $\sim 100$  nm to  $\sim 3\mu\text{m}$ ) and spheroidal oligomers ( $\sim 20$ - $80\text{nm}$ ) (Fig. 3.3, Fig.3.4, and Fig.3.5). Native PAGE experiments confirmed the formation of both low and high molecular weight assembled structures (Fig 3.2).

**Table 3.1.** List of several pathophysiological conditions linked to phenylketonuria with detailed metabolic alterations.

Pathophysiology linked to PKU	Metabolic alterations
Cerebral deficiency	Reduced dopamine and serotonin concentration in blood(Surtees and Blau 2000)
Neuronal dysfunction and <i>dementia</i>	Reduces dopaminergic and serotonergic metabolites in CSF as well as decreased catecholamine and serotonin concentrations in the brain(McKean 1972).
Oxidative stress, lipid and protein oxidative damage	Deficiency of L-carnitine(Sitta, Barschak, et al. 2009).
CNS lesions with demyelination	Elevated S-100B protein in serum(Kleopatra H Schulpis et al. 2004).
Coronary Heart disease, neurological disorder	Low serum cholesterol, HDL,LDL and high triglycerides and VLDL(Sherpa et al. 2011).
Increase adiposity	Elevation of leptin plasma levels(K H Schulpis et al. 2000).
Mutation	DNA damage in leukocytes(Sitta, Manfredini, et al. 2009).
Neurotoxicity	Reduced acetylcholinesterase activity in erythrocyte membranes(Tsakiris et al. 2002).
Neurotoxicity, uremia, <i>rheumatoid arthritis, diabetes mellitus</i> , essential hypertension, spongiform encephalopathy.	Reduces the activities of Na,K-ATPase and Mg <sup>2+</sup> -ATPase in erythrocyte membranes(Kleopatra H Schulpis et al. 2002).
Enhance oxidation stress, Lipid oxidation	Ubiquinone 10 (Q10) deficiency in lymphocytes(Artuch et al. 2001).
Interfere with cholesterol biosynthetic pathway	Inhibition of enzyme 3-hydroxy-3-methylglutaryl CoA reductase.

**Table 3.2.** List of selected amyloid linked diseases induced by peptide sequences that contains aromatic residues including phenylalanine.

Name of parent peptide/protein	Pathophysiological conditions	Short active Sequence*
Islet amyloid polypeptide	Diabetes mellitus (type II diabetes)	FGAIL(Tenidis et al. 2000)
$\beta$ -Amyloid peptide	Alzheimer's disease	QKLVFF,LPFFD, LVFFA(Mark A. Findeis et al. 1999)(Pallitto et al. 1999).
lactadherin	Aortic medial amyloid	NFGSVQFV(Häggqvist et al. 1999)
Gelsolin	Finnish hereditary amyloidosis	SFNNGDCCFILD(Gazit 2002)
Serum amyloid A	Chronic inflammation amyloidosis	SFFSFLGEAFD(Bemporad 2006)
Thyroid carcinoma peptide	Thyroid carcinoma	DFNKF, DFNK(Reches et al. 2002)
Human muscle acylphosphatase amyloid	Human muscle acylphosphatase	RVQGVCFRMTEDEAR SKLEYSNFSIRY(Westermark et al. 1992)
Calcitonin	Medullary thyroid carcinoma	YTQDFNKKFFHTFPPQTAIGV(Benvenga et al. 1994)(Berger et al. 1988)
BRI	Neuronal dysfunction and dementia	FENKFAV FAIRHF(Vidal et al. 1999)
$\beta$ 2-microglobulin	Dialysis-associated renal amyloidosis	DWSFYLLYTEFT(Jones et al. n.d.)

\*Phenylalanine is indicated in red color fonts and other aromatic residues are represented in green color fonts.

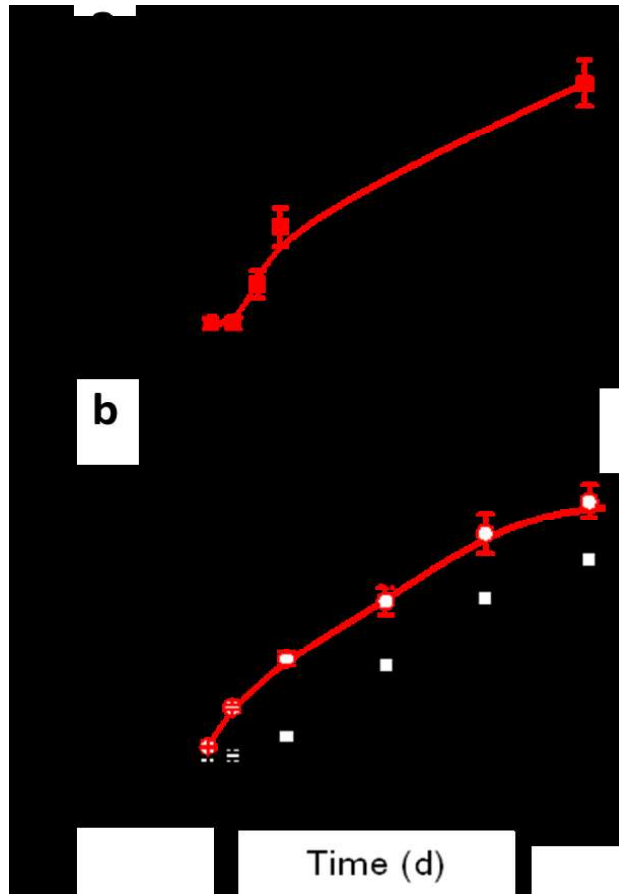


**Figure 3.1. Phenylalanine-aggregates in physiological conditions.** **a**, Increase in Thioflavin T signal of 6 mM phenylalanine sample in PBS at pH 7.4. **b**, A self-seeded aggregation reaction of phenylalanine.

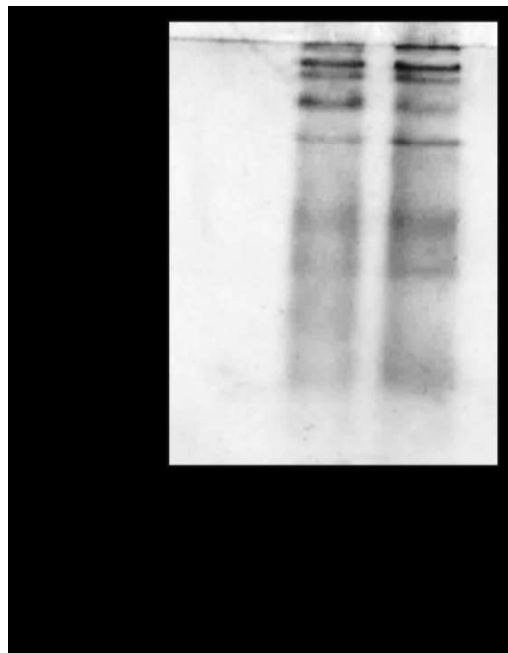


**Figure 3.2:** Self-assembly of phenylalanine into higher order structures, as resolved by Native PAGE.

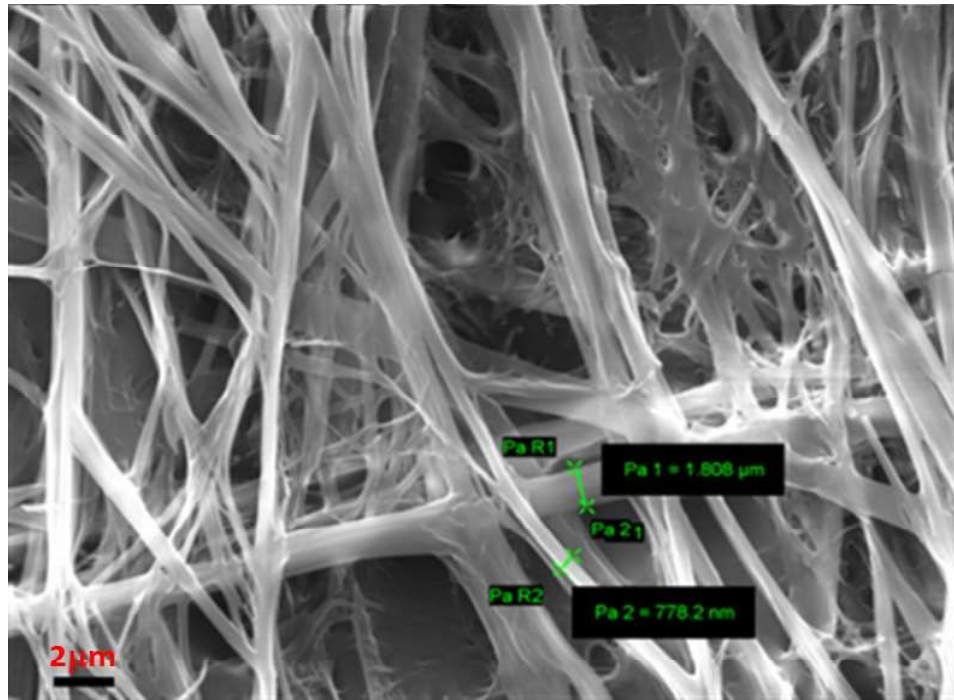


**Figure 3.3:** SEM images, representing regular fibrils of phenylalanine sample aggregated in water at 37°C. Scale bar, ~2 μm.

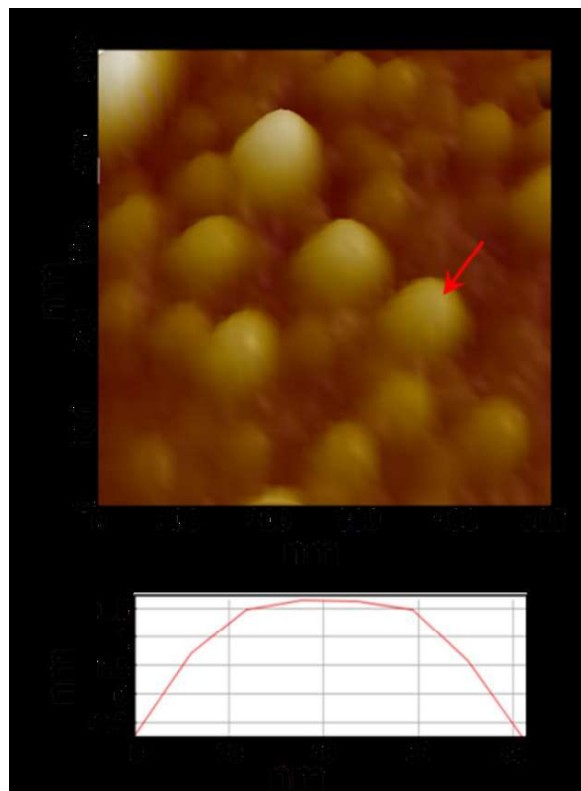


**Figure 3.4.** AFM image, representing spheroidal oligomers of phenylalanine sample aggregated at 37°C. The diameter range was from ~25nm-80nm.

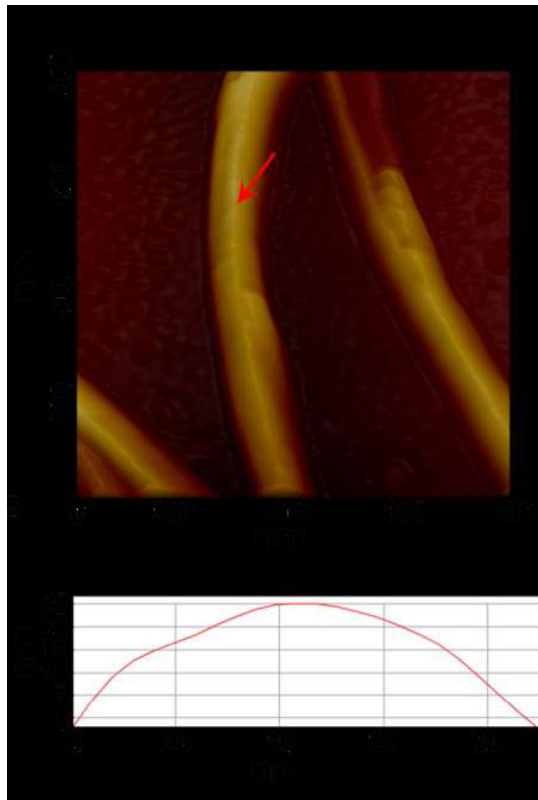


**Figure 3.5.** AFM image, representing regular fibrils of phenylalanine sample aggregated in water at 37°C. The diameter range was between ~100nm-160nm.

### 3.1.2: Effect of phenylalanine aggregates on aggregation properties of selected globular proteins.

Since several globular proteins co-exist in the body, the question of what effect phenylalanine fibrils would have on the aggregation propensity of these proteins, particularly those ones that exist in the blood, is very significant. To address this critical question, samples consisting of mixed soluble monomers of selected globular proteins (lysozyme + serum albumin + insulin + myoglobin + cytochrome c) which are commonly found in the blood (Table 3.3) were incubated under *in vitro* conditions both in the presence and in the absence of phe-fibrils. The curiosity was whether the phe-fibrils have the potential to trigger the aggregation of globular proteins. All the aggregation reactions were performed in PBS (pH 7.4) at 37°C to mimic a physiological condition. In the presence of phenylalanine fibrils (~15% w/w), the mixed monomer sample showed an increase in the Thioflavin T signal, suggesting the conversion of soluble monomers of proteins into amyloid like higher order structures (Fig 3.6). To further clarify this seeding effect of phenylalanine-fibril, its effect on individual proteins was examined and the results indicated a gradual increase in the Thioflavin T signal to a saturation point, confirming the amyloid formation of individual proteins (Fig. 3.6 and Fig. 3.7). Without phenylalanine seeds, control aggregation reactions of both isolated monomers and mixed monomers did not show any indication of aggregation (Fig. 3.6). From the preceding results, it is evident that phenylalanine-fibrils can effectively trigger an aggregation process in proteins under physiological conditions in which proteins usually retain their soluble native states. This observation is further supported by previous studies on cross-seeding among proteins or peptides during amyloid formation (Kar et al. 2014)(Dubey et al. 2014a).

**Table 3.3.** Physiological concentration of the blood proteins, their functions and related pathophysiology.

Protein	Overview about the protein	Function	Protein pathophysiology	Relevance to PKU
BSA	Most abundant serum protein, MW-66.5 kDa, Synthesis site liver (12-25gm/day), Half-life – 16 hrs, Reference range in body -3.5 to 5.5 g/dL	Blood coagulation, transports hormones, fatty acids, drugs etc., Maintains oncotic pressure, prevents photodegradation of folic acid	Peripheral and pulmonary edema delayed wound healing (MacKay and Miller 2003) Nephrotic syndrome, hepatic cirrhosis, heart failure and malnutrition(Garcia-Martinez et al. 2013a)	Coronary Heart disease, malnutrition
Insulin	Synthesized in the pancreas within the $\beta$ -cells of the islets of Langerhans. MW-5.8 kDa, half life 4-5 hrs Reference range in body – Fasting- < 25 mIU/L 30 minutes after glucose - 30-230 mIU/L 1hrs after glucose -18-276 mIU/L 2hrs after glucose -16-166 mIU/L 3hrs or more after glucose -< 25 mIU/L	Carbohydrate and fat metabolism, facilitates the packing of glucose into fat cells as triglycerides,	Localized amyloid deposition <sup>35</sup> , poor glycemic control, acanthosis nigricans, hyperinsulinemia is directly related to Cancer, Obesity, type-II diabetes, Hypertension (Kopf et al. 2001), Arthrosclerosis(Hansen et al. 2013), Chronic inflammation, cardio vascular disease (Eschwège 2003), prostate enlargement etc.	Type-II diabetes, cardio vascular disease, amyloid deposition
Cyt c	Located in the mitochondrial intermembrane. MW- 12kDa, half-life 5 to 8 minutes	Electron transport, intrinsic type II apoptosis, scavenges reactive oxygen species, oxidizes cardiolipin during apoptosis	Lewy bodies and other neurodegenerative disorders(Hashimoto et al. 1999)	Neurodegenerative disorders
Lysozyme	synthesis in osteoclasts MW- 14.3 kDa, half-life 4hrs Reference rang in body – In serum -7-13 mg/l In tears about 120 times higher than in serum In urine about 8 time more than in serum	Hydrolyzing the glycosidic bond, Immune functions.	Prominent amyloid nephropathy, nephrotic syndrome and sicca syndrome(Valleix et al. 2002), spontaneous splenic rupture, cholestasis, and liver failure, massive hepatic hemorrhage	
Myoglobin	Synthesis in cardiac myocytes and oxidative skeletal muscle fibers. MW 16.7 kDa, half life	Oxygen storage, serve as a buffer of intracellular $PO_2$ , Facilitated $O_2$ diffusion, scavenger of NO in heart, normal muscle development and function	Muscular dystrophy, rhabdomyolysis(Hendgen-Cotta et al. 2010)	

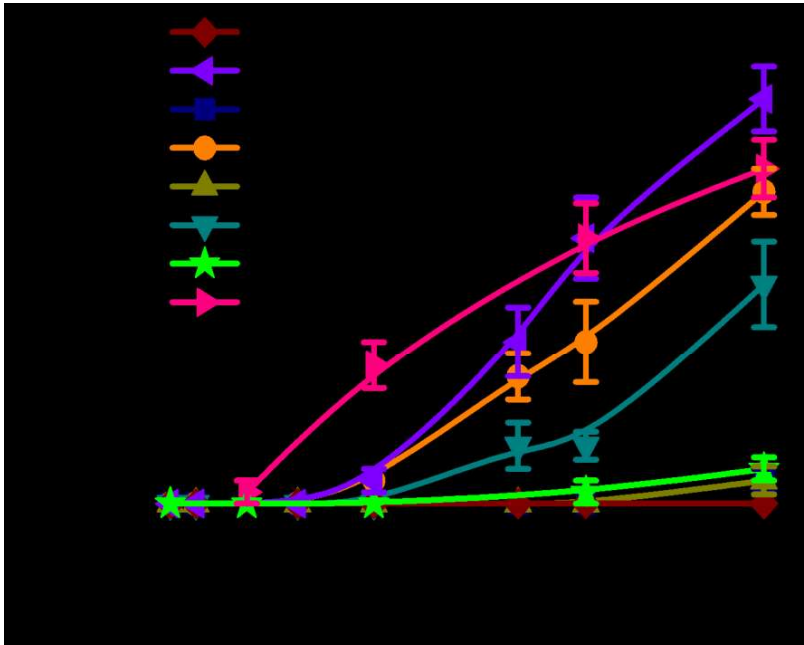


**Figure 3.6.** Thioflavin T signals revealing rapid aggregation and coaggregation of globular proteins driven by phenylalanine-fibrils (present at 15% w/w seeds) as labeled.

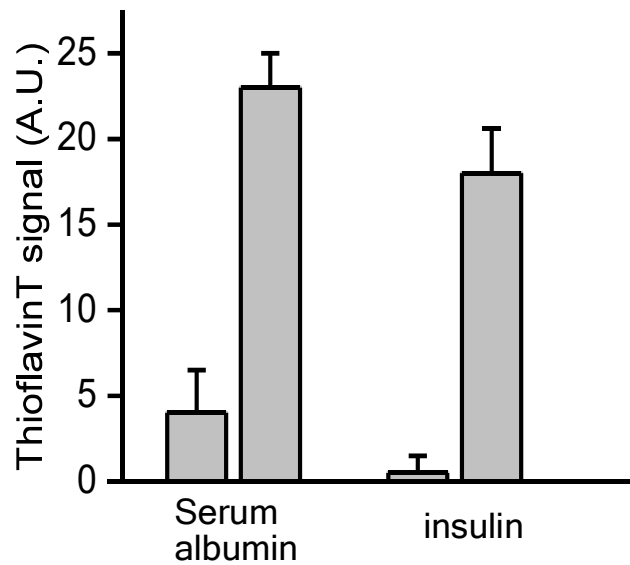


**Figure 3.7.** Histogram showing Thioflavin T signals of insulin and BSA at 0 h and 24 h in the presence of phenylalanine fibrils.



### 3.1.3: Structural characterization of protein amyloid fibrils obtained from phenylalanine-driven aggregation reaction

To throw light on this surprising phenylalanine-induced protein aggregation process, native PAGE experiments were conducted which revealed the presence of both mature aggregates and stable oligomers (Fig. 3.8). Next, circular dichroism (CD) measurements were carried out and the CD profiles clearly indicated conformational switch towards  $\beta$ -sheet structures (Fig. 3.9a, Table 3.4). Formation of  $\beta$ -structured species after protein aggregation was further confirmed by FTIR data (Fig. 3.9b). The self-assembly of proteins driven by phenylalanine-fibrils yielded different supramolecular assembled structures including cylindrical microfibrils and twisted flat tapes (Hall et al. 2016)(Ridgley and Barone 2013) (Fig. 3.10, 3.11, 3.12, 3.13 and 3.14), as evident from SEM studies. Notably, the morphologies of the fibrils obtained from either mixed monomers or from individual monomers were found to be similar. To further unravel the distinct features of the higher order structures of these proteins, AFM images were examined which showed the occurrence of both mature regular fibrils and spheroidal oligomers (Fig. 3.15 and 3.16). The results obtained from the native PAGE of mature aggregates (Fig. 3.8) were found to correlate well with the data obtained from SEM and AFM experiments (Fig. 3.10 and 3.16, Fig.3.12 to Fig. 3.16), particularly revealing the occurrence of both mature fibrils (100nm-3 $\mu$ m) and oligomeric species (~20-80 nm).

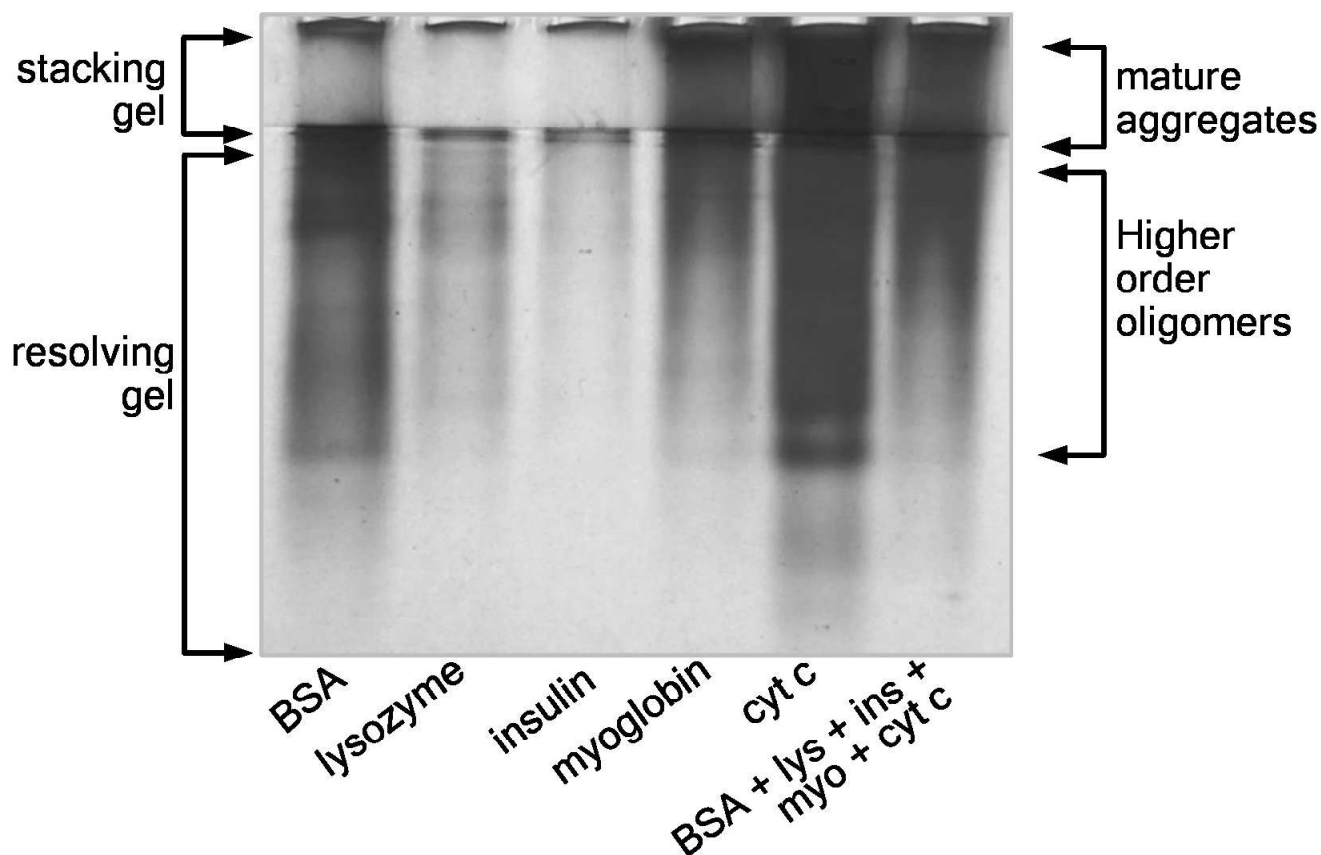


**Figure 3.8** Native PAGE of protein samples confirming aggregation of globular proteins triggered by phenylalanine-fibrils.

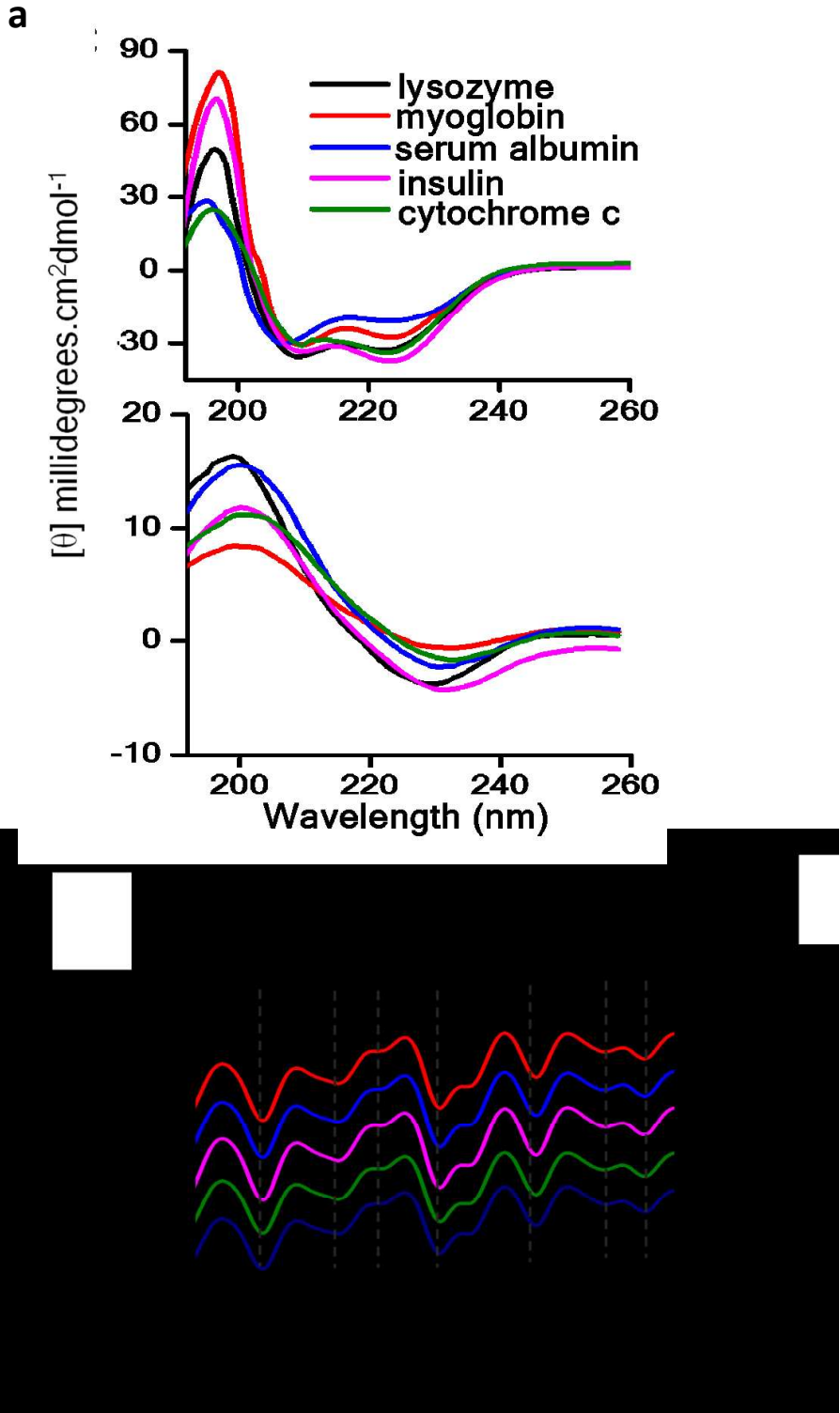


**Figure 3.9 Structural characterization of higher order structures of proteins obtained from phenylalanine-driven aggregation.** a) Circular dichroism spectra of proteins, showing a conformational switch towards  $\beta$ -sheet structure. b) ATR-FTIR spectral signals of mature protein fibrils indicating the dominance of  $\beta$ -structured species, as labelled.

**Table 3.4.** Predicted secondary structures of protein samples before and after aggregation using circular dichroism data. K2D3 online tool(Louis-Jeune et al. 2012) was used to theoretically predict the secondary structures of protein samples.

Samples	Soluble Proteins		Aggregated Proteins	
	$\alpha$ -helices (%)	$\beta$ -sheets (%)	$\alpha$ -helices (%)	$\beta$ -sheets (%)
BSA	68 $\pm$ 3	9 $\pm$ 2	2 $\pm$ 1	34 $\pm$ 2
Lysozyme	35 $\pm$ 1	17 $\pm$ 3	1 $\pm$ 1	43 $\pm$ 3
Insulin	33 $\pm$ 2	19 $\pm$ 2	3 $\pm$ 1	33 $\pm$ 3
Myoglobin	85 $\pm$ 2	0 $\pm$ 1	3 $\pm$ 1	43 $\pm$ 3
Cytochrome c	78 $\pm$ 1	0 $\pm$ 1	3 $\pm$ 1	42 $\pm$ 2

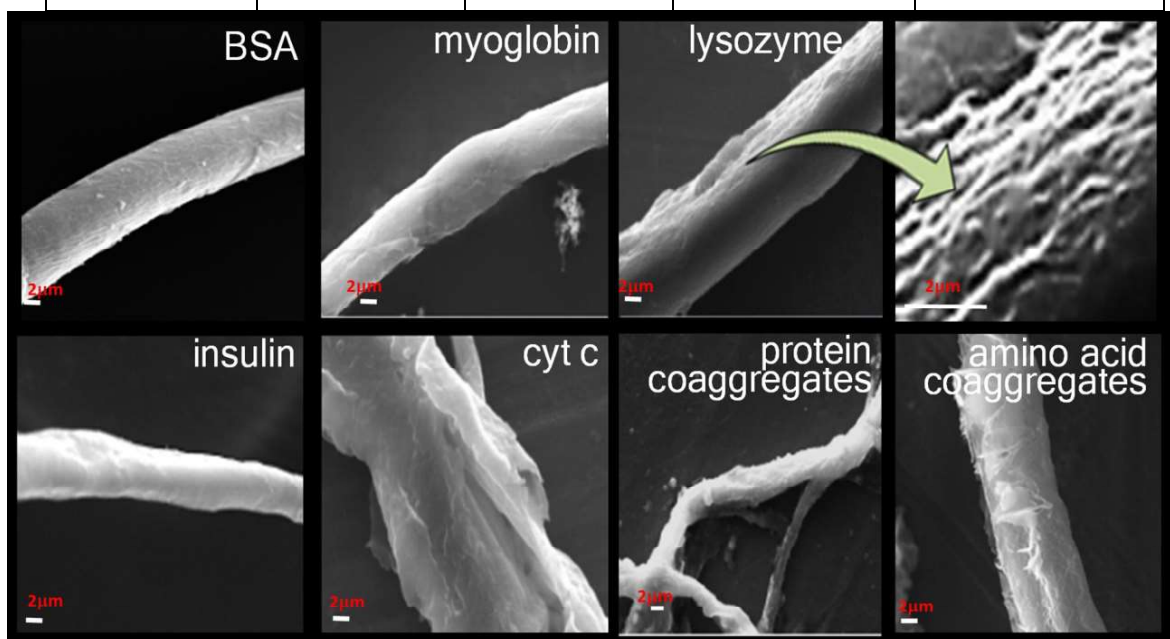


**Figure 3.10** SEM images of mature fibrils of different proteins. Scale bar, 2  $\mu$ m.

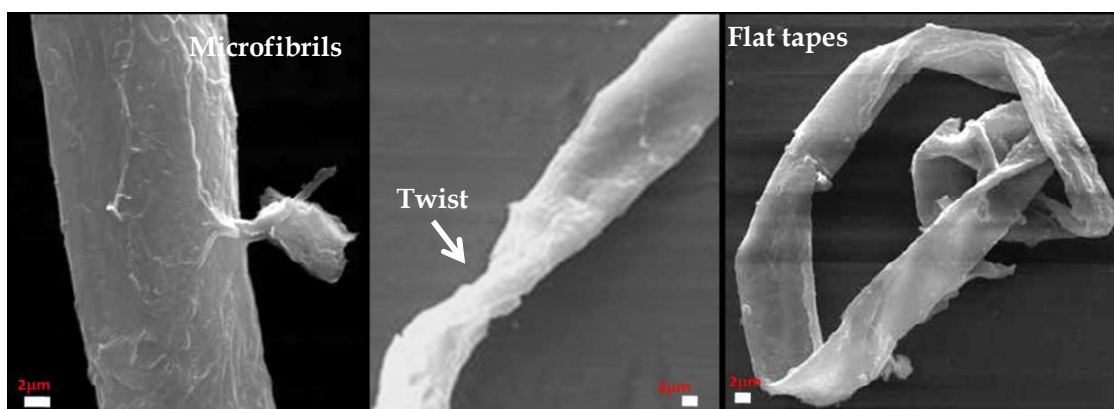


**Figure 3.11.** SEM images representing different morphologies of BSA aggregates. Scale bar,  $\sim$ 2  $\mu$ m.

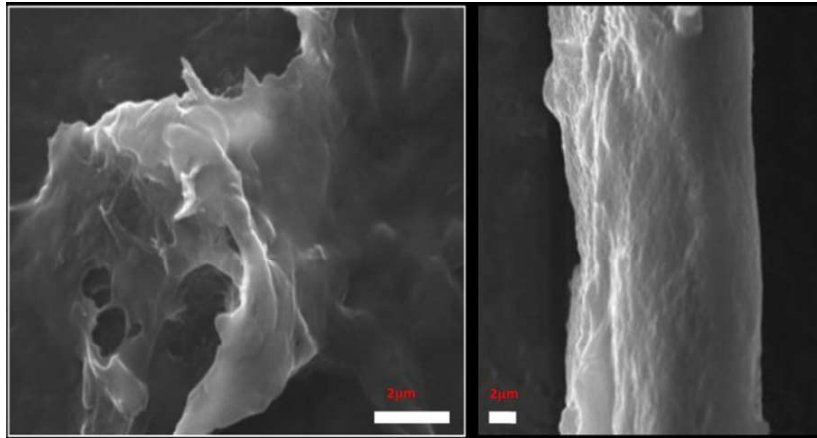


**Figure 3.12.** SEM images representing different morphologies of lysozyme aggregates. Scale bar,  $\sim 2 \mu\text{m}$ .

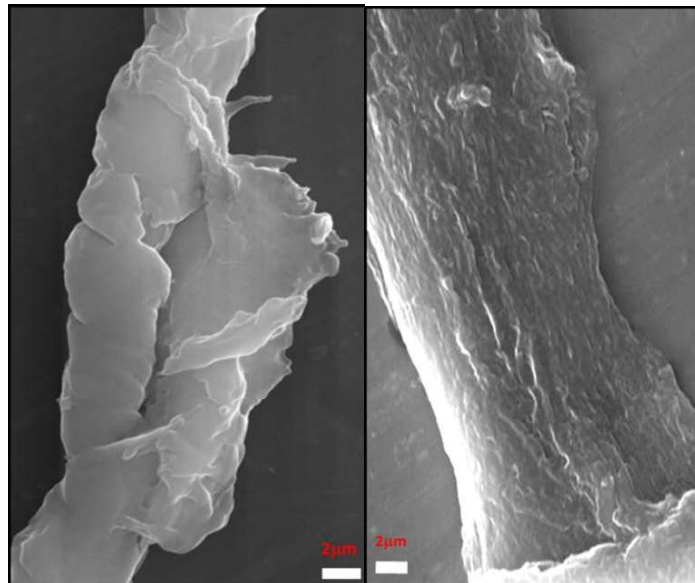


**Figure 3.13.** SEM images representing different morphologies of myoglobin aggregates. Scale bar,  $\sim 2 \mu\text{m}$ .

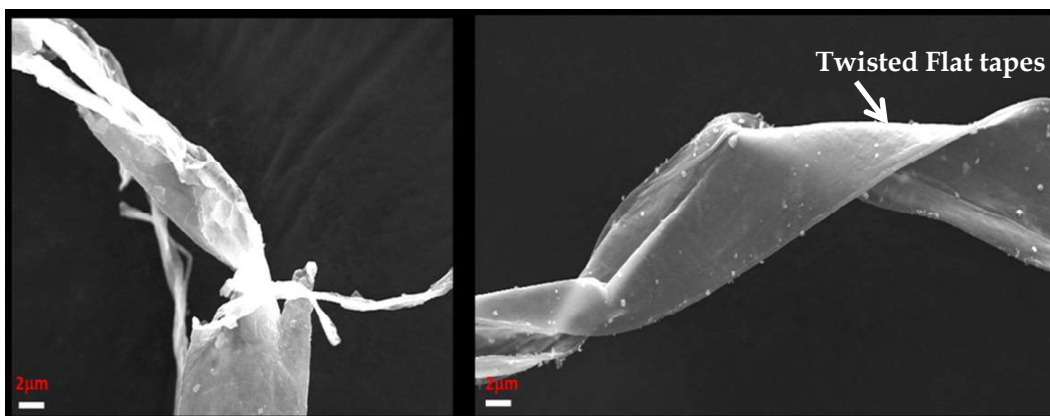


**Figure 3.14.** SEM images representing different morphologies of insulin aggregates. Scale bar,  $\sim 2 \mu\text{m}$ .

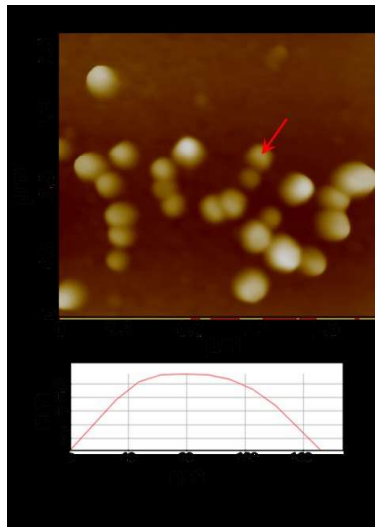


**Figure 3.15.** AFM image, representing spheroidal oligomers (within 150-200 nm) observed in phenylalanine induced aggregation of mixed protein monomers (in PBS at 37°C).

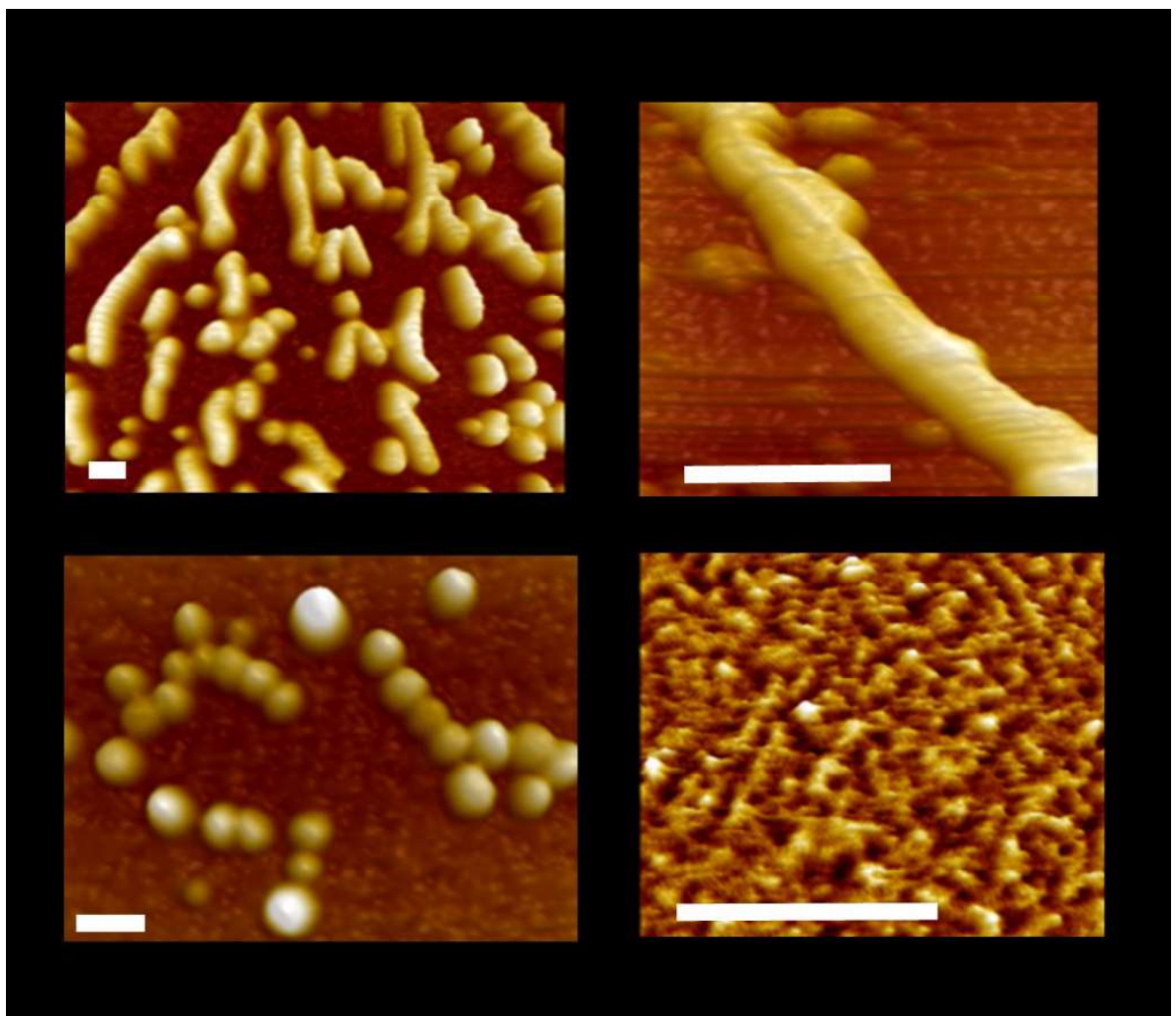


**Figure 3.16** AFM images, representing microfibrils (150-200 nm) observed during phenylalanine induced aggregation of mixed protein monomers (in PBS at 37°C). Scale bar 100 nm.



### 3.1.4: Effect of phenylalanine aggregates on amino acids.

Since earlier studies have demonstrated the occurrence of spontaneous aggregation of single amino acids under extreme temperature conditions (Singh et al. 2014)(Shaham-Niv et al. 2015), it was examined whether the phenylalanine-fibrils can drive any such aggregation process of amino acids under physiological conditions. When an aliquot of phenylalanine-fibrils was added to a soluble mixture of amino acids, the sample underwent an aggressive aggregation without any lag phase (Fig.3.17), mimicking a self-seeded aggregation reaction of phenylalanine (Fig. 3.1b). Examination of these amino acid-generated fibrils by AFM and SEM showed formation of linear fibrils that shared a similar morphology with the protein fibrils (Fig. 3.10, Fig. 3.19). The resultant fibrils generated from aggregation of amino acids were also found to be Thioflavin T positive, confirming the presence of amyloid like structures (Fig. 3.18).

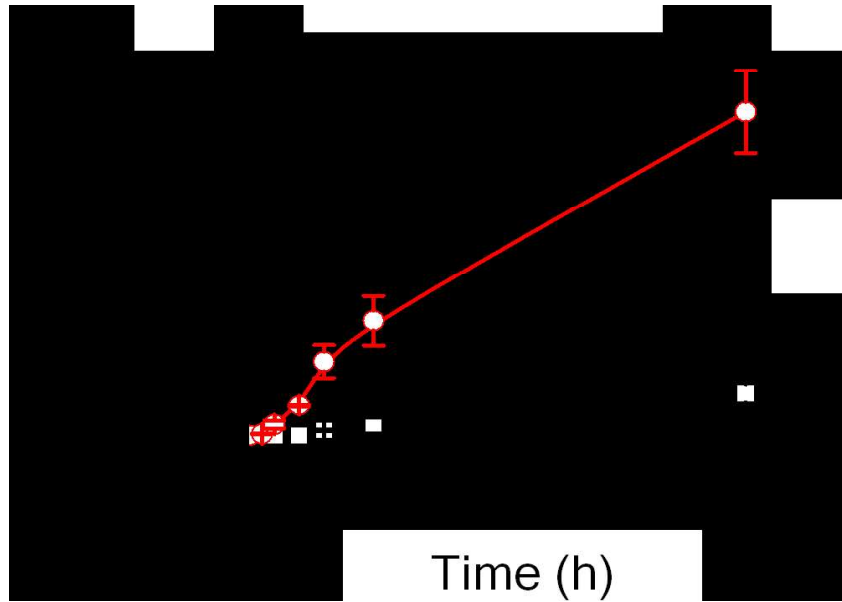


**Figure 3.17** Turbidity data showing aggregation of a soluble mixture of amino acids (Tyr + Trp + Phe + Glu + Arg + Ala), driven by phenylalanine-fibrils

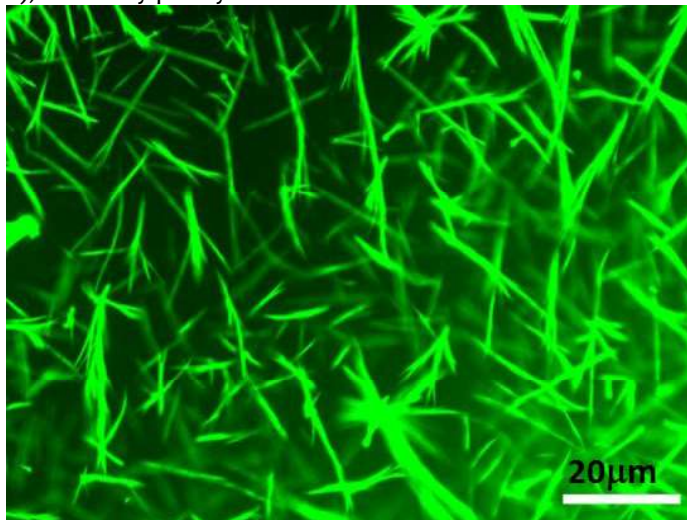


**Figure 3.18.** Optical images of fluorescent self-assembled nanostructures (stained with an amyloid specific dye Thioflavin T) generated from a phenylalanine-induced aggregation reaction of a soluble mixture of amino acids (in PBS at 37°C). Scale bar, 20µm.

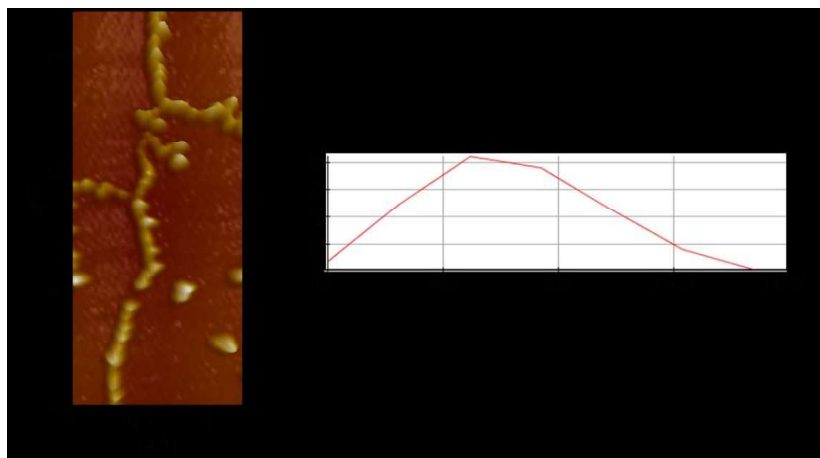


**Figure 3.19.** AFM image of higher order structures obtained for phenylalanine-induced aggregation of mixed amino-acids (in PBS, 37°C).

### 3.1.5: Does Phenylalanine fibrils and phenylalanine-induced protein fibrils have any effect on hemolysis?

Having established the inherent ability of the phenylalanine-fibrils to trap soluble globular proteins as well as amino acids into an aggregation pathway that generates  $\beta$ -structured amyloid like entities, further experiments were carried out to know whether these fibrils have any damaging effect on vital blood components, particularly on the RBCs. Since anaemia, a condition caused by lysis of RBCs, is one of the most striking severities found in PKU patients (Ruppert 1967), unravelling the hemolytic effect of these aggregates would be highly relevant to improve the mechanistic understanding of PKU. Hence, hemolytic assays were performed using RBCs collected from the blood sample of a healthy volunteer. Phenylalanine, in its soluble state, did not trigger lysis of RBCs, as evident from SEM (Fig 3.25a) and optical microscopy images (Fig 3.21). However, strong lysis of RBCs was observed in the presence of phenylalanine fibrils (Fig 3.25a, Fig. 3.21). Notably, a time-dependent deformation of intact RBCs using dark field microscopy (Fig. 3.24)

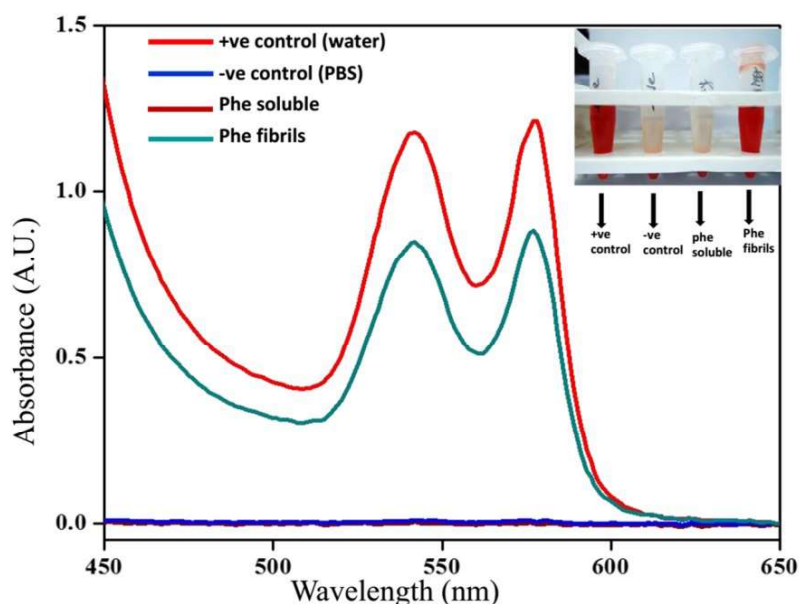
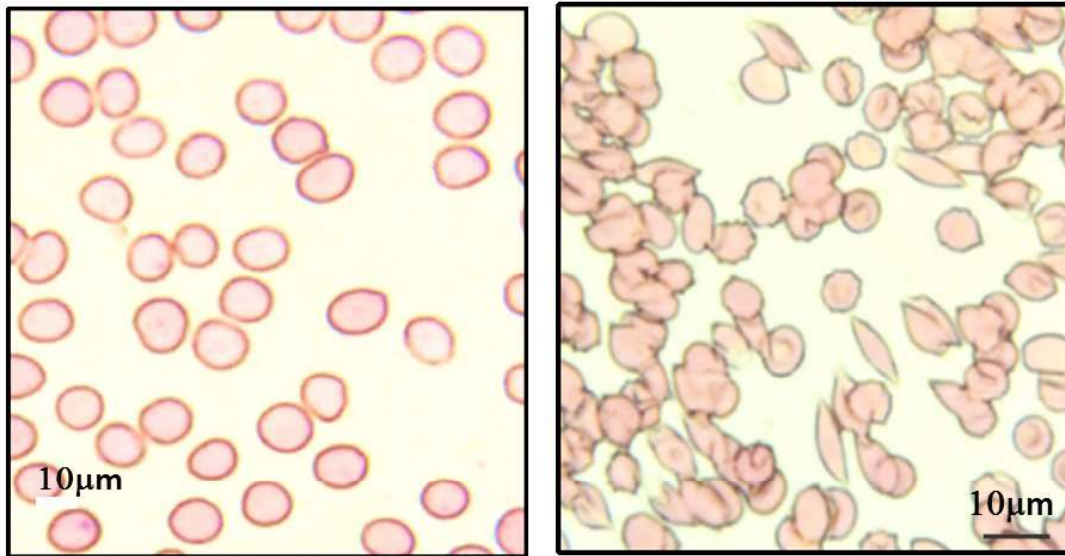


**Figure 3.20.** UV absorption spectra obtained for the hemolysis experiment after four hours of incubation at 37°C. Severe lysis was observed in the presence of water (+ve control) and phenylalanine fibrils whereas no lysis was detected in the presence of soluble phenylalanine and in PBS buffer (used as –ve control).



**RBCs + soluble Phe**

**RBCs + Phe fibrils**

**Figure 3.21** Optical microscopy images of normal RBCs in the presence of soluble phenylalanine and lysed RBCs in the presence of phenylalanine-fibrils.

**Table 3.5.** Percentage hemolysis of RBC's in the presence of different soluble and aggregated samples of proteins.

Sample	Concentration	% lysis of RBCs in the presence of soluble sample	% lysis of RBCs, in the presence of aggregated sample
Phenylalanine	~6mM	0	53.0
BSA	~13µM	0	20.0
Insulin	~156µM	0	45.0
Lysozyme	~63µM	0	16.5
Cytochrome c	~74µM	0	19.9
Myoglobin	~51µM	0	18.8
Co-aggregates	~1.8µM	0	19.0



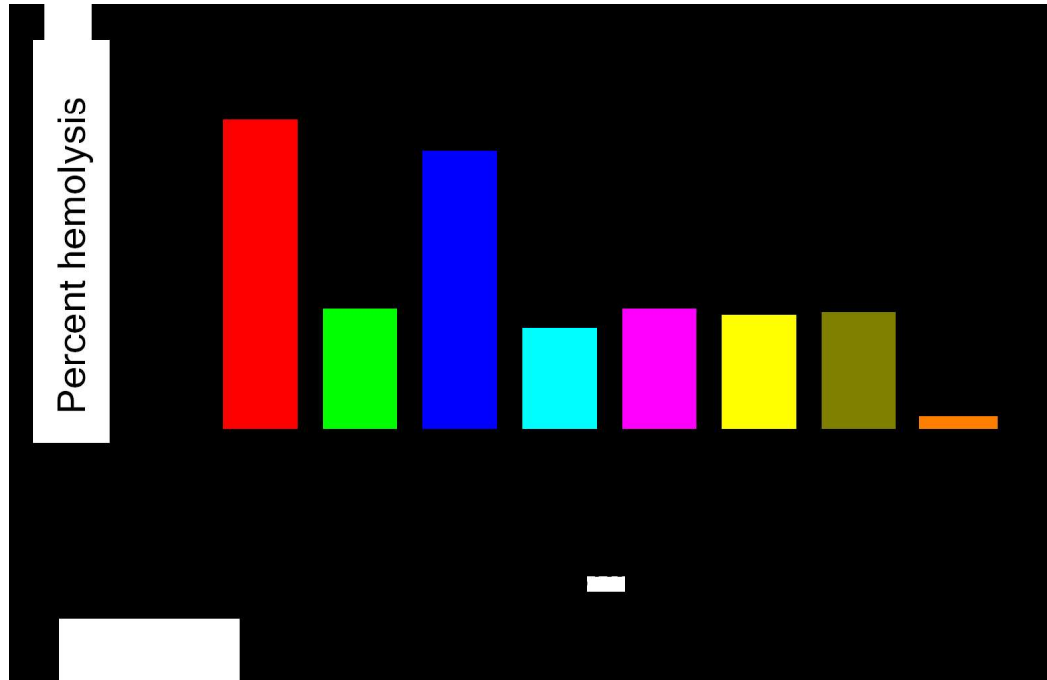


**Figure 3.22** Histograms showing the percentage hemolysis

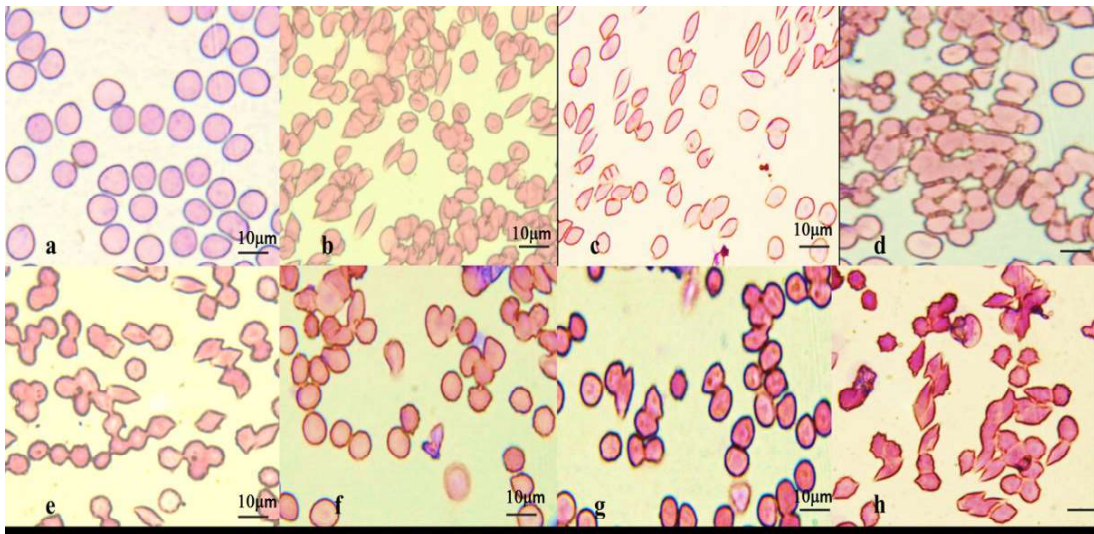


**Figure 3.23.** Leishman stained images of RBCs, visualized by the light microscope (Leica DM 500 Switzerland), in the presence of: a) PBS (control RBCs) b) Phenylalanine aggregates c) BSA aggregates d) Insulin aggregates f) Lysozyme aggregates g) Cytochrome C aggregates h) Myoglobin aggregates i) aggregates of mixed protein monomers.

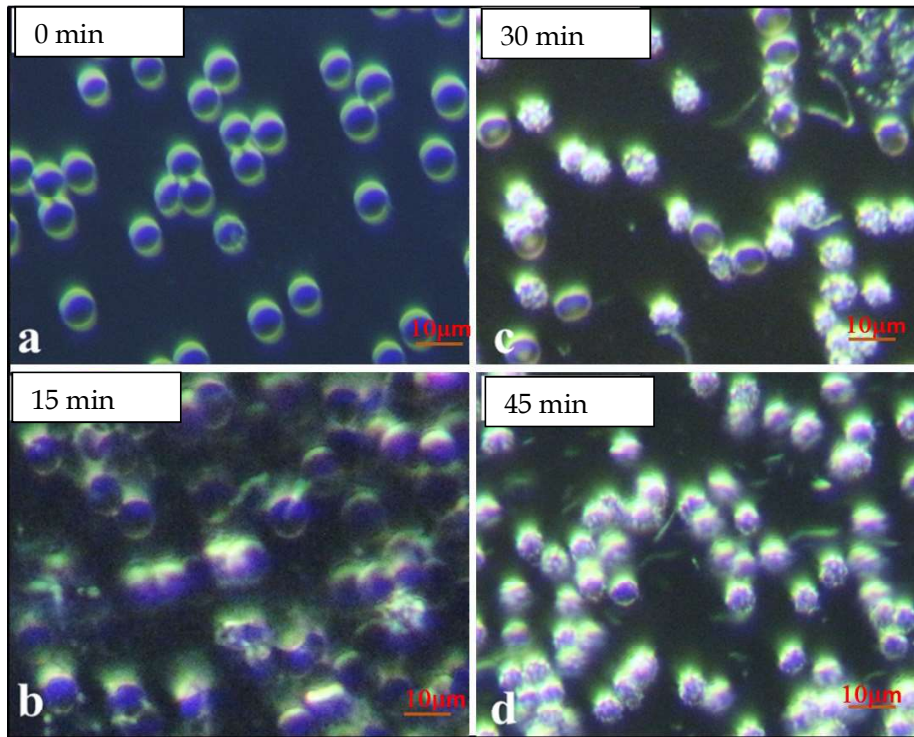


**Figure 3.24.** Dark field microscopy images showing time dependent live imaging of RBC's during lysis caused by phenylalanine fibrils.

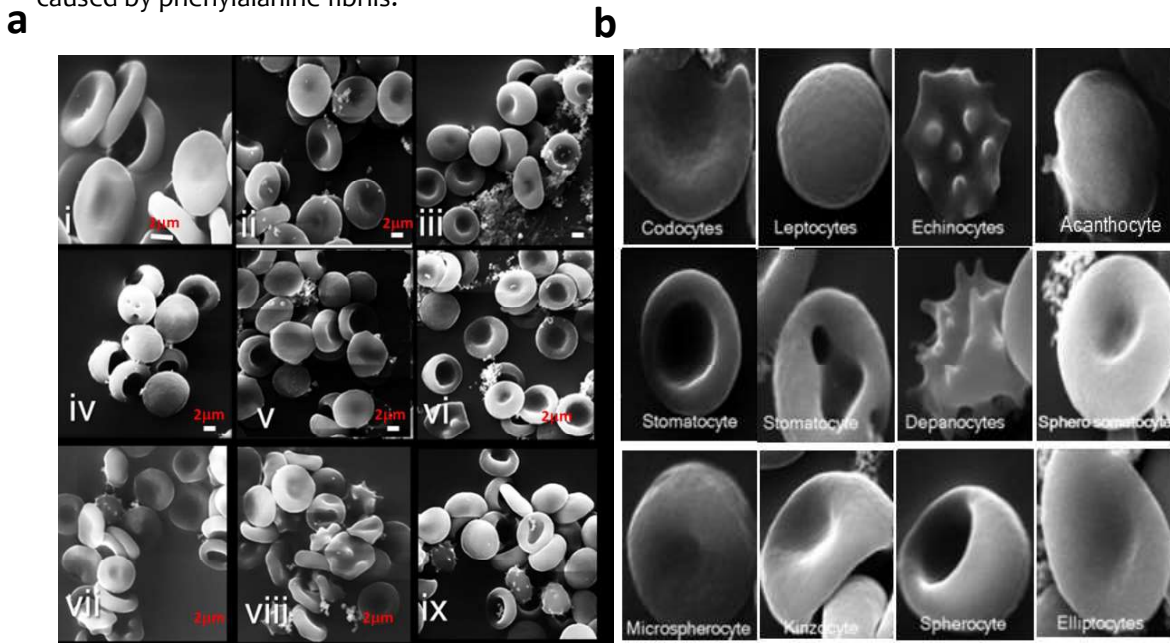


**Figure 3.25.** Phenylalanine fibrils and phenylalanine-induced protein fibrils trigger hemolysis. a, SEM images of RBCs in the presence of: (i) 1X PBS, (ii) soluble Phe (iii) Phe-fibrils (iv) BSA fibrils, (v) lysozyme fibrils (vi) insulin fibrils (vii) myoglobin fibrils (viii) cytochrome c fibrils (ix) Coaggregation generated fibrils. All protein fibrils are obtained from phenylalanine fibril-seeded reactions. Scale bar, 2µm. b, Selected SEM images of damaged RBCs revealing the occurrence of pathological deformability.

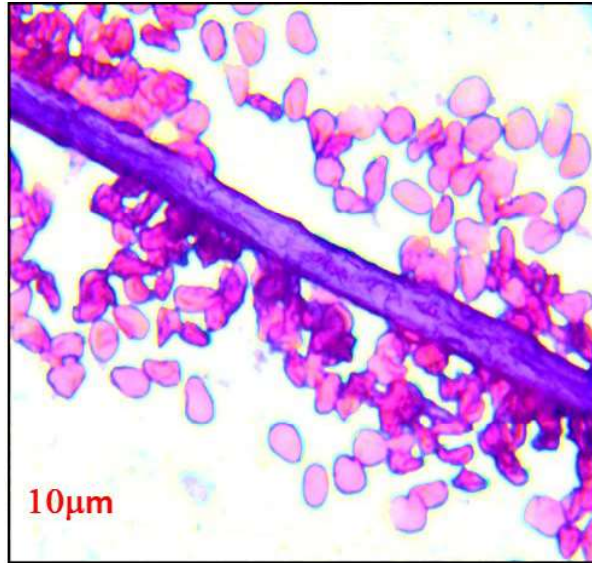


**Figure 3.26.** Leishman stained microscopic image showing adherence of lysed-RBC's to the surface of protein fibrils

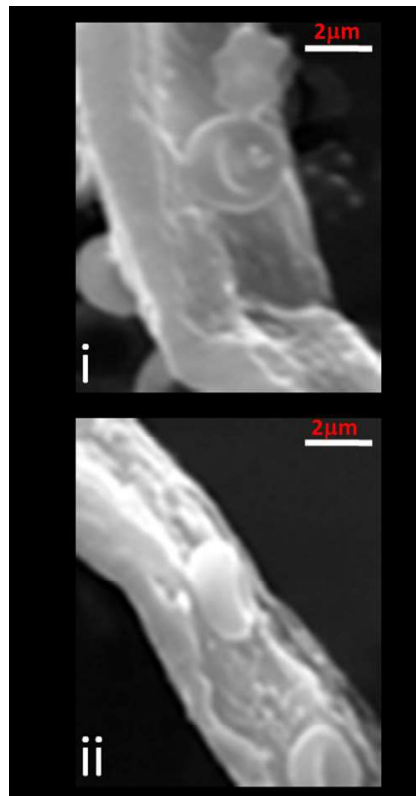


**Figure 3.27.** SEM images showing adherence of lysed-RBC's to the surface of protein fibrils. Scale bar, ~2 μm.

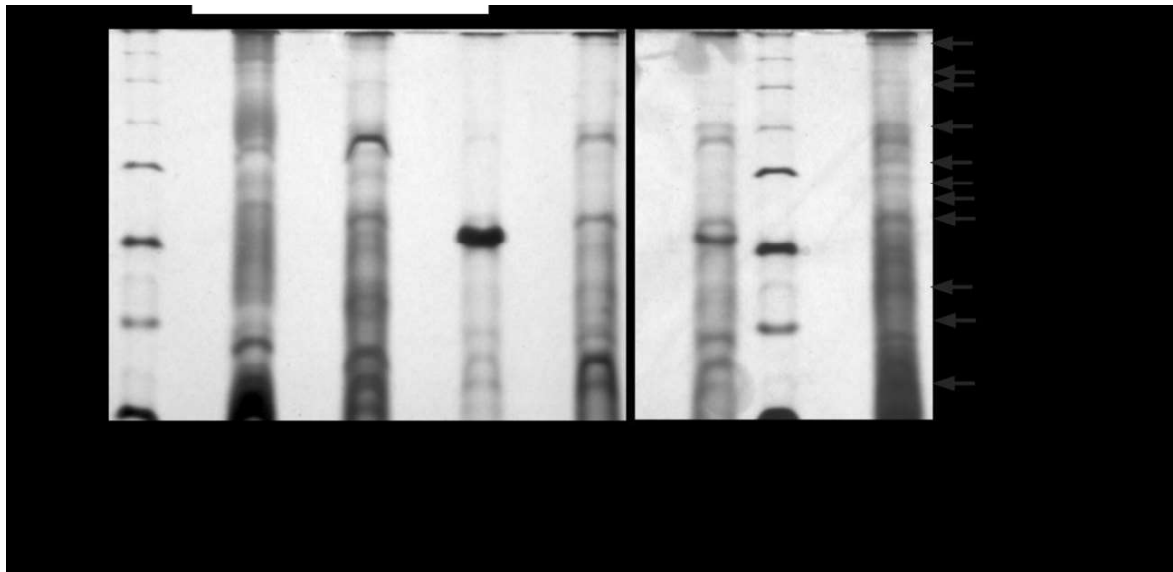


**Figure 3.28** Analysis of lysed erythrocyte membrane proteins as labelled using silver-stained SDS-PAGE.

**Table 3.6** List of diseases related to deformability of RBCs (Bessis 1974)(Bessis 1977).

Shapes of Erythrocytes	Linked Pathophysiology
Acanthocytes	Abetalipoproteinemia cirrhosis and rarely other liver diseases
Codocytes	Thalassemia
Leptocytes	Hypochromic anemia
Echinocytes	Uremia, Congenital anemia
Echinodacrocytes	Thalassemia, hemolytic anemia with Heniz bodies
Microspherocytes	hereditary Spherocytosis and somatocytosis
Somatocytes	Hereditary or acquired hemolytic anemia
Elliptocytes	Congenital elliptocytosis
Kinzocytes	Hemolytic anemia and hereditary Spherocytosis
Spherocytes	hereditary Spherocytosis, burns and some hemolytic anemia
Depanocytes	Sickle celled anemia
Sphero somatocytes	hereditary Spherocytosis and somatocytosis

This result validates the inherent ability of phenylalanine-fibrils to trigger hemolysis. Interestingly, all the phenylalanine-induced protein aggregates also showed similar haemolytic effect (Fig 3.23, and Fig. 3.25a). SEM revealed a plethora of different deformed RBCs which were identified as acanthocytes, codocytes, leptocytes, echinocytes, echinodacrocytes, microspherocytes, somatocytes, elliptocytes, kinzocytes, spherocytes, epanocytes, and spherosomatocytes (Fig 3.25b and Table 3.6). The results clearly prove that fibril samples, obtained from both individual aggregations as well as from coaggregation, were toxic to RBCs. The percentage of lysis caused by phenylalanine-fibrils was observed to be ~50% (Fig. 3.22, Fig. 3.20), whereas more than ~20% lysis was observed in the presence of all protein aggregates except insulin aggregates which showed more intense lysis of ~ 45%. When the effect of



phenylalanine fibrils on hemolysis was tested at a concentration value that was used for seeding the protein aggregation reactions, a negligible (~1.9%) lysis was detected (Fig. 3.22). Hence, in this experiment the observed toxicity was due to the presence of protein amyloids. To examine the release of different membrane proteins during lysis of RBCs, SDS-PAGE was performed using the lysed RBCs in the presence of both phenylalanine-fibrils and phenylalanine-induced protein fibrils. SDS-PAGE revealed several distinct protein bands (Fig. 3.28), confirming the presence of various surface proteins of lysed RBCs(Murphy et al. 2004).

### 3.1.6: Molecular simulation of phenylalanine assembly and molecular docking studies of phenylalanine with proteins.

To understand the intermolecular interactions during self-assembly of phenylalanine, molecular dynamics simulation studies were conducted. Phenylalanine molecules were simulated in a cubic box model at 37°C by DS4 (Fig.3.28). The result revealed that the phenylalanine molecules have an inherent property to form well organized self-assembled tubular like structure (Guo et al. 2016) comprising a hydrophobic exterior and a hydrophilic interior (Fig 3.29 c). The self-assembly of phenylalanine molecules was facilitated by viable hydrogen bonds and  $\pi$ - $\pi$  interactions (Fig.3.30). The molecular docking studies of phenylalanine with proteins viz BSA, Insulin, Lysozyme, Cytochrome C and Myoglobin has shown its binding affinity for globular proteins, as evident from the docking studies (Fig. 3.31 to Fig. 3.35).

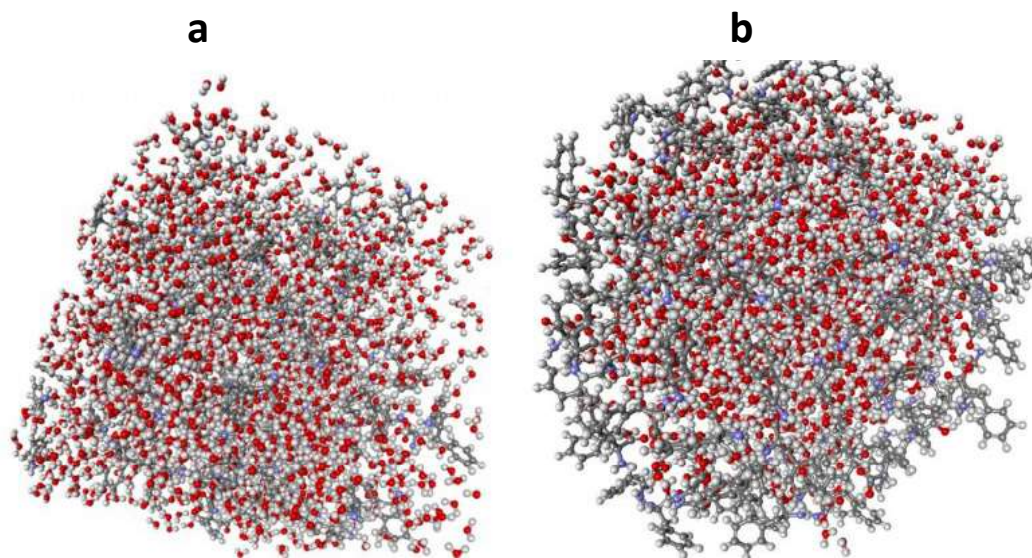


**Figure 3.29.** Phenylalanine molecules before (a) and after (b) molecular dynamics studies.

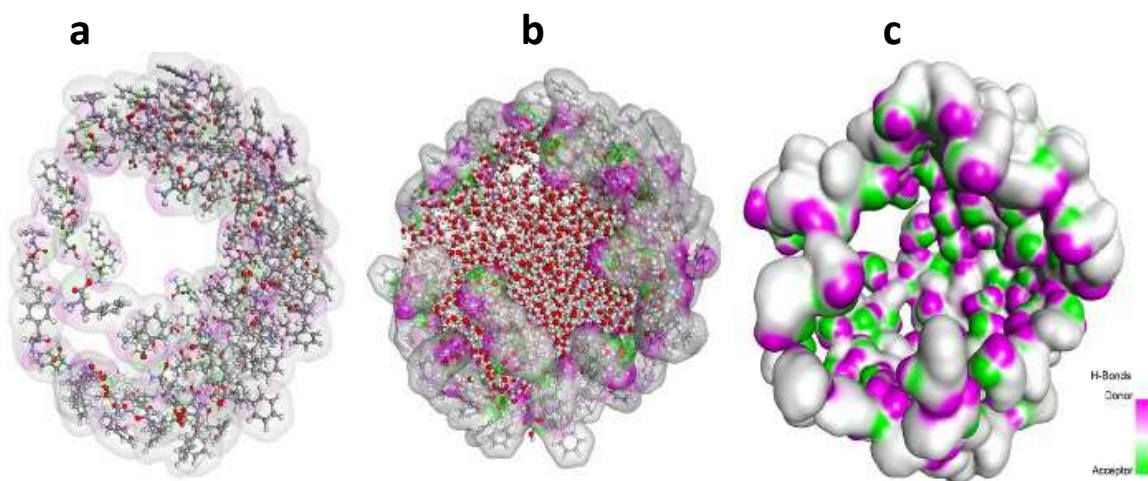


**FIGURE 3.30. Molecular simulation study reveals self-assembly of phenylalanine residues.** (a) Tubular assembled higher order entities. (b) The packing of water molecules within the inner core of the structure. (c) Space filling model of the structure revealing the presence of both acceptor and donor functional groups for hydrogen bond formation.

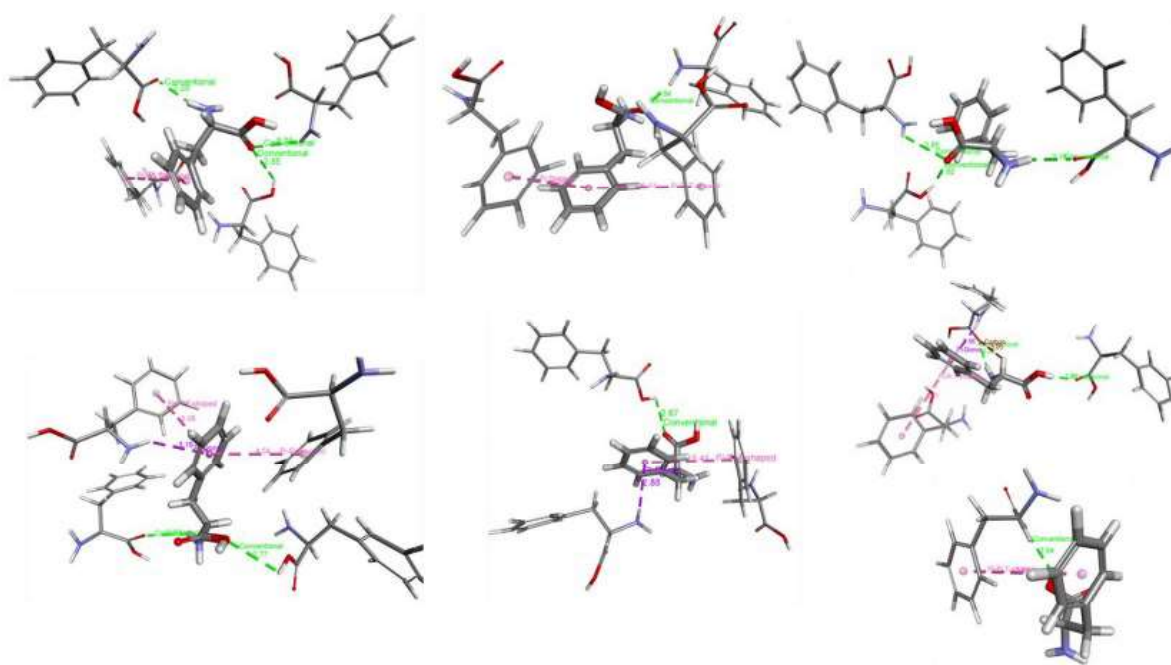


**Figure 3.31** Possible interaction of phenylalanine molecules with each other.

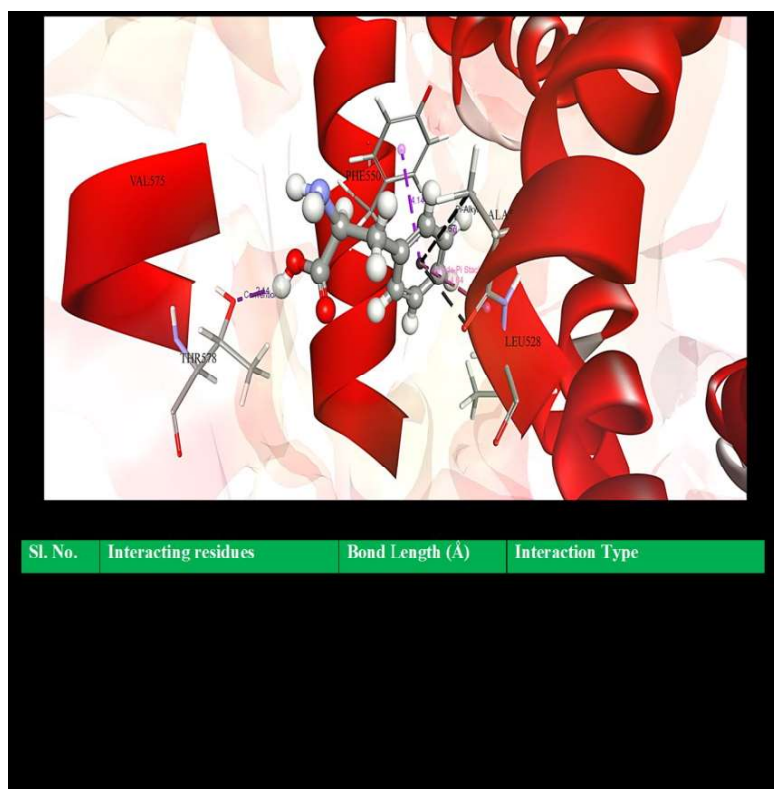


**Figure 3.32.** Summary of Bovine Serum Albumin PDB: 4F5S–Phenylalanine interaction. The value of – CDOCKER energy was 27.0621 kcal mol<sup>-1</sup> and the value of – CDOCKER interaction energy was found to be 28.9882 kcal mol<sup>-1</sup>.

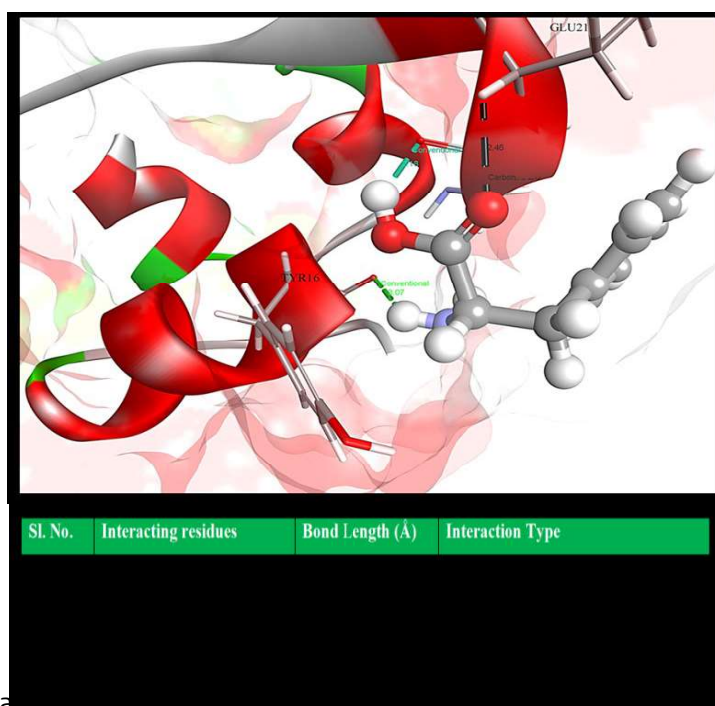


**Figure 3.33.** Summary of Bovine Serum Albumin PDB: 4F5S–Phenylalanine interaction. The value of – CDOCKER energy was 14.3516 kcal mol<sup>-1</sup> and the value of – CDOCKER interaction energy was found to be 14.3759 kcal mol<sup>-1</sup>.





**Figure 3.34.** Summary of Lysozyme PDB 193L–Phenylalanine interaction. The value of – CDOCKER energy was 26.8447 kcal mol<sup>-1</sup> and the value of – CDOCKER interaction energy was found to be 29.0785 kcal mol<sup>-1</sup>.

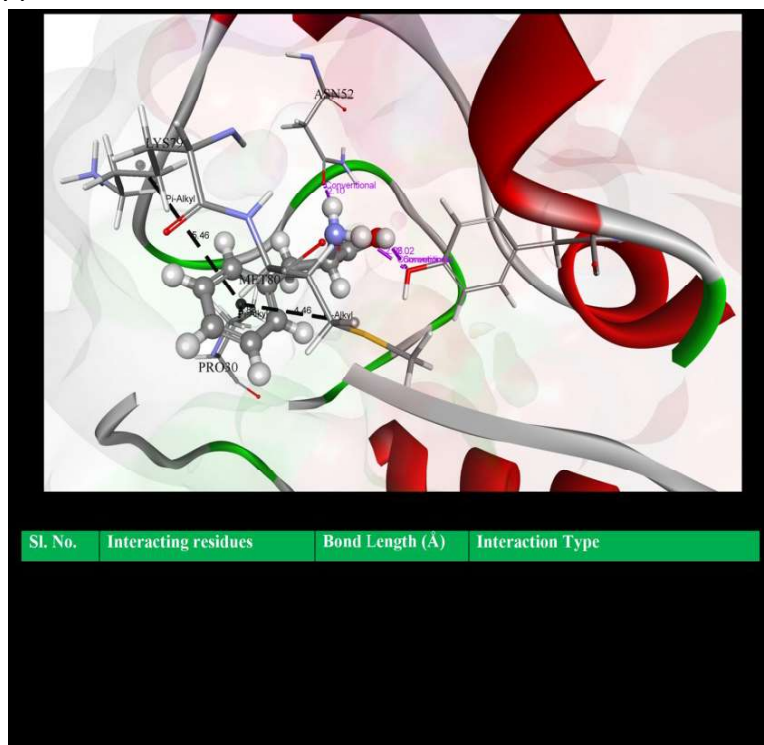


**Figure 3.35.** Summary of Cytochrome C PDB: 1HRC–Phenylalanine interaction. The value of – CDOCKER energy was 26.4082 kcal mol<sup>-1</sup> and the value of – CDOCKER interaction energy was found to be 28.6882 kcal mol<sup>-1</sup>.



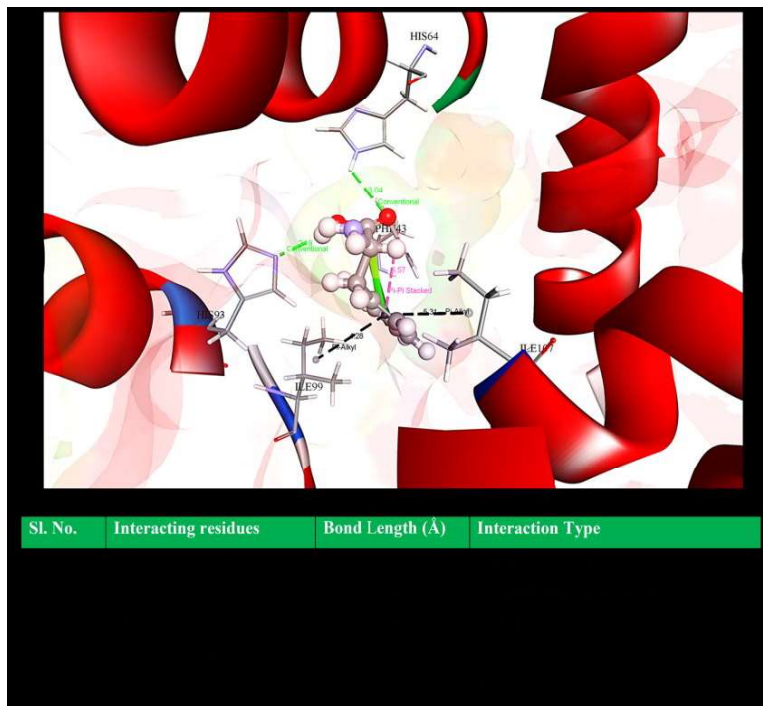


**Figure 3.36.** Summary of Myoglobin PDB: 1DWR–Phenylalanine interaction. The value of –CDOCKER energy was 22.615 kcal mol<sup>-1</sup> and the value of –CDOCKER interaction energy was found to be 24.6064 kcal mol<sup>-1</sup>.

### 3.2 DISCUSSION

These experimental findings provide insight into two inherent properties of phenylalanine that appear highly relevant to PKU: (i) phenylalanine fibrils form a lethal aggregation trap for proteins and amino acids under physiological conditions; and (ii) both phenylalanine fibrils and phenylalanine-induced protein fibrils were found to be highly toxic to RBCs.

The vast medical significance of deformed RBCs (Table 3.6) proposes a direct link between hemolysis and phenylketonuria (Ruppert 1967). Under normal conditions, RBCs maintain a unique biconcave discoidal shape (Toumey 2011), however the origin of RBC-deformability is clinically attributed to the onset of hemolysis (Rother et al. 2007) and sometimes to predispose hypoxia (Nakagawa et al. 2011). The damaging effect of amyloid-RBC interaction is known to cause deformability and oxidative reduction in RBC (Nakagawa et al. 2011) (Jayakumar et al. 2003) (Mattson et al. 1997a). Interestingly, in this work, in addition to hemolytic effect, a striking tendency of lysed-RBCs to adhere to the surface of phenylalanine-fibrils or proteins-fibrils (Fig. 3.26 and Fig. 3.27) was observed. Higher hydrophobicity of amyloid fibrils is known to promote its intervention with RBC bilayer (Pillot et al. 1996). On the other hand, strong interaction between hydrophilic core of phenylalanine oligomers with the cell membrane has been reported to induce cellular damage through ion leakage (Do et al. 2015a).

The simulation studies on Phe molecules suggest the formation of supramolecular arrangement of Phe molecules resulting in a structure comprising of a hydrophobic exterior and a hydrophilic interior (Figure 3.29). The self-assembly of phenylalanine molecules was facilitated by viable hydrogen bonds and pi-pi interactions (Figure 3.30). Formation of similar higher order structures with hydrophobic exterior and hydrophilic interior has been reported

earlier for amyloid fibrils (Perutz et al. 2002). Hence, in its amyloid-like higher order entities (Do et al. 2015b)(Singh et al. 2014)(Adler-Abramovich et al. 2012), phenylalanine is predicted to preferentially interact with the membrane components of RBCs (Nakagawa et al. 2011)(Ulrich et al. 1999) through viable hydrophobic and electrostatic interactions (Do et al. 2015c).

The result from the docking studies revealed that the phenylalanine molecules have an inherent affinity for globular proteins( figure 3.32, 3.33, 3.34, 3.35 and 3.36. It is much likely that such crucial phenylalanine-protein interactions would be preferentially favoured when the zwitterionic phenylalanine molecules are arranged within the fibrillar entities (Do et al. 2015a)(Adler-Abramovich et al. 2012)(German et al. 2015). Adherence of proteins to the surface of the phenylalanine fibrils may reflect two consequences: (i) a conformational switch towards an aggregation-prone state, and (ii) a preferred intermolecular association between such aggregation-prone species due to increase in the local concentration of such species.



Phenylalanine  
induced  
hemolysis

**Figure 3.37.** Schematic outline of the summary of the current investigation.

### 3.3. CONCLUSION

This study confirms the hemolytic effect of phenylalanine-fibrils, which can effectively trap proteins into an aggregation pathway, that is predicted to reduce the normal protein levels causing several protein deficiency diseases (Garcia-Martinez et al. 2013b)(Sonksen and Sonksen 2000)(Hanley et al. 1970) (Table 3.3), while accumulating neurotoxic protein amyloids(Ross and Poirier 2004). Since anemia and several neuronal-disorders are highly prevalent in patients with PKU, the findings of this work on the ability of both phenylalanine fibrils and phenylalanine-induced protein fibrils to trigger hemolysis may be of great clinical significance.

...